

Temperature Sensor Coursework Report

Imperial College London, Dep. of Electrical and Electronic Engineering, ELEC70101 - Sensors,
Group 7: Henry Milne, Tadas Ramancevicius, Ulvi Babyev, Mehwish, Bhatti

1. Introduction

In this laboratory exercise, 4 different temperature sensor types were characterised: a digital one-wire sensor (*DS18B20*), an RTD sensor (*PT1000*), an analogue sensor (*TMP36*), and an IR sensor (*MLX90614*). It is important to note that the first three sensors are contact-based, while the fourth one is contactless. Characterisation encompasses parameters such as accuracy, precision, sensitivity, linearity, response time, hysteresis, and more. The target characterisation range was 0-100°C. Custom test benches were built to evaluate the sensors under controlled conditions.

2. Test Benches

2.1. Above-Room-Temperature Test Bench, Contact

Sweeping the voltage of a 12V Heating Element provides the above room temperature testing range ranging from laboratory temperature (~20°C to ~60°C). Thermal paste was applied onto the Heating Element (enough of it to fully submerge the sensor). Third Hands secure the sensor in position - this removes displacement-related errors.

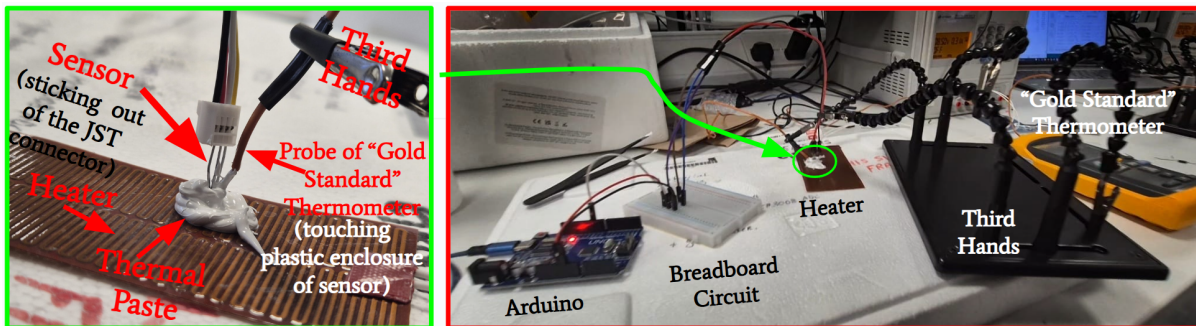


Figure 1. Test Bench for temperatures above room temperature

Note that the sweeps are carried out in both directions, i.e., from room temperature (~20°C) to ~70°C, and from ~70°C to room temperature. Though note that although the maximum temperature produced by the Heating Element was 70°C (at 12V), the packages of the sensors placed onto it only reached around 60°C. Therefore, the probe of the "Gold Standard" thermometer must be positioned in a way that it is contacting the packaging of the sensor, but not the surface of the Heating Element itself to give a more accurate reference value. Outputs of both the sensor under test and the Fluke 52 II "Gold Standard" thermometer were recorded while conducting sweeps.

2.2. Below-Room-Temperature Test Bench, Contact

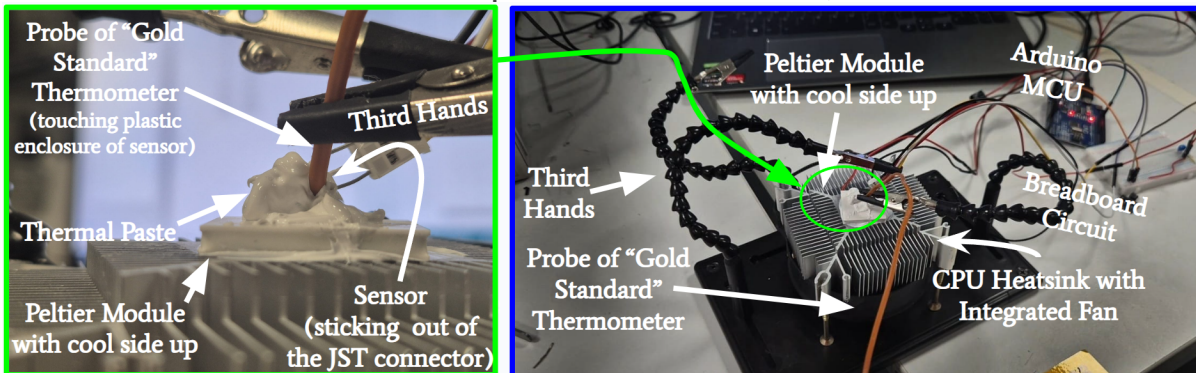


Figure 2. Test Bench for temperatures below room temperature.

A CPU fan and heatsink is raised upside down on stilts. A Peltier module is placed on top of the heatsink with the hot side facing down onto the heatsink, this is interfaced with thermal paste for an

efficient thermal junction. The cold side of the Peltier faces upwards and provides a temperature range of 0°C to room temperature (~20°C) when the supply voltage is swept from 0V to 3V. Thermal paste was applied onto the cold side of the Peltier (enough of it to fully submerge the sensor). Third Hands secure the sensor in position - this removes displacement-related errors. Outputs of both the sensor under test and the Fluke 52 II “Gold Standard” thermometer were recorded while conducting sweeps.

2.3. Contact Test Bench Characterisation Challenges

Thermal Resistance between Sensor and Heater/Cooler: Thermal resistance was addressed using a thermal paste with a high conductivity of 1.8W/m·K (RS PRO 2024). Due to its viscosity, it fills in gaps between surfaces and provides much better heat transfer. As such, this was used whenever an efficient thermal junction was needed between solids.

Thermal Loading of Heater/Cooler by Sensor: For this test bench, thermal loading would not pose an issue since temperature sweeps from room temperature are performed, and settling time is allowed. This means that the Heater/Peltier and the sensor will have come to an equilibrium and should maintain steady temperatures when measurements are being taken.

Joule Heating of Sensor: Joule heating of the digital sensor was mitigated by ensuring that the sampling interval was large enough to prevent excessive heating and allowing time for the sensor to cool in between measurements. The analogue sensor’s current draw is just 0.05mA (Analog Devices 2015) so any self-heating would be negligible. The RTD sensor also has a relatively low current draw of 0.2mA (Heraeus Sensor Technology, n.d.). Also, due to the design of the sensor being enclosed within a metal housing, this would better dissipate any temperature gain resulting from joule heating into the thermal mass of the rest of the test bench setup. The circuitry for each sensor is explained in more detail in later sections.

Convection: The fan of the Peltier module’s heatsink blows air upwards, past the testing area, and so could impact the temperatures recorded. As such a low RPM on the fan was used, except when it was necessary to increase the cooling of the hot side of the Peltier module as we got to colder temperatures.

Radiation: In the test bench, the Fluke and contact sensor being assessed were held in place, touching each other deep within a large volume of thermal paste. This meant that any temperature gradient created as a result of heat radiating off the surface of the thermal paste should be negligible in the distance between the “Gold Standard” thermometer and contact sensor.

2.4. Cooling Test Bench (from 80°C to 20°C), Contactless

The initial test bench consisted of a beaker and a CPU fan to accelerate cooling, but the setup proved highly susceptible to air currents and radiative disturbances.

The MLX90614 utilises the radiated heat flux according to the Stefan-Boltzmann law to produce results: $q = \epsilon\sigma(T_s^4 - T_o^4)$. Although the MLX90614 uses an optical filter to block visible light (wavelength passband 5.5-14μm), radiative disturbances can still affect the measurement (Melexis 2013).

To mitigate these effects, the beaker was completely encased in a black duct tape, which absorbs incident radiation and minimises unwanted reflections. However, this also extended the duration of the cooling experiment (~70 °C to ~20 °C) to over two hours. To minimise the duration, a Peltier cooler was introduced underneath the beaker (making direct contact with the glass), reducing experiment time to one hour. Additional measures, including the use of Third Hands and a cardboard cutout lid, were employed to minimise movement of the IR sensor (as small movements or variations in the sensor’s angle of incidence were found to introduce measurable error) and the probe of the “Gold Standard” thermometer.

The sensor leads were extended so that it could be suspended inside the beaker with a restricted field of view. Boiled water was poured into the beaker, thermal paste was applied between the glass and the Peltier module, and temperatures were logged every 10-15s via an Arduino MCU. This procedure was repeated three times to assess repeatability.

Although the new test bench improved measurement consistency, it still had limitations. During the initial setup, hot steam was able to escape freely; however, with the top of the beaker covered, steam built up and caused shorts in the sensor's wiring, resulting in multiple breakages. Additionally, the test bench did not maintain the IR in the same position after each run due to degradation of the cardboard, resulting in perturbations in each result and affecting precision.

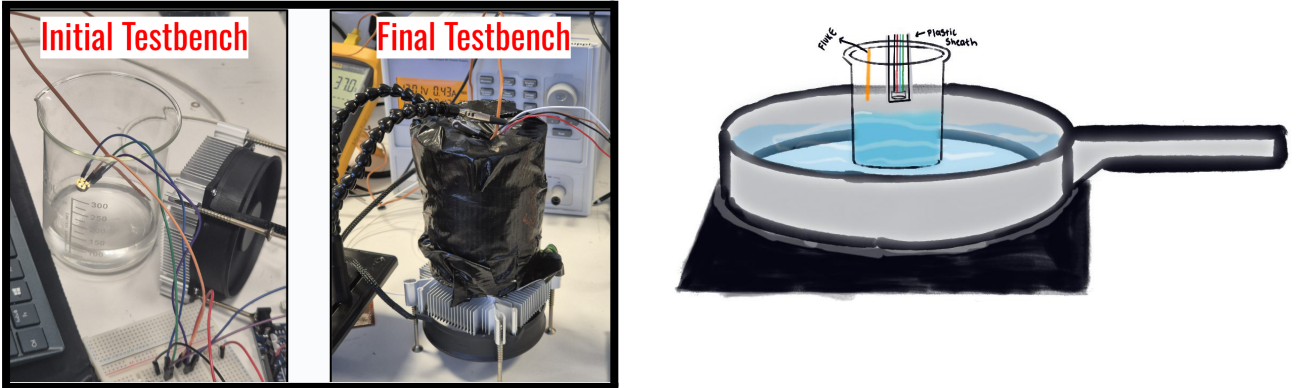


Figure 3. LEFT: Cooling test bench (2.4); RIGHT: Heating test bench (2.5)

2.5. Heating Test Bench (from 0°C to 80°C), Contactless

This test bench followed a setup similar to the previous one. A saucepan containing a small amount of water was placed on an induction stove. The beaker was placed into this water-filled saucepan. This setup ensured even heat distribution across the beaker's base, preventing thermal stress that could otherwise damage the beaker. The beaker contained a large quantity of ice and was heated gently to protect the insulating material. The IR sensor and the "Gold Standard" probe were positioned as before, and measurements were taken three times. Initial readings from the gold standard were unstable due to the pulsed heating of induction stoves. To improve reliability, measurements were cross-checked with a glass thermometer as a secondary reference, and the beaker was gently stirred. The highest temperature observed was recorded, corresponding closely with the readings from the glass thermometer. This approach demonstrated better accuracy and precision in the results.

To provide protection from steam, a plastic sheath was used for the thermometer, as it was sufficiently transparent to the long-wavelength range that the sensor operated at.

2.6. Additional Notes

Note that the developed test benches are relatively cost-effective, with the total cost of components (excluding ones provided for the exercise by the department) used being less than £25. They are also power efficient due to, for example, the use of thermal paste, which allows them to reach more extreme temperatures at a given input power (as discussed previously). Lastly, in terms of safety risks, the most notable ones are the >70°C temperatures of boiling water and the Heating Element, as well as the use of water in proximity to electronic devices - extra care was taken throughout the lab work.

3. Hardware

3.1. MCU Choice & ADC

With permission from the coursework leader, the microcontrollers used for this lab exercise were the Arduino Uno and Arduino Mega 2560 instead of the provided Raspberry Pi 3B+. There are two reasons for this. Firstly, group members had more experience and were more comfortable with programming Arduino MCUs. Secondly, the Raspberry Pi would have been more complex to set up due to the Wi-Fi interface.

The analogue (*TMP36*) and the RTD (*PT1000*) sensors both output an analogue voltage and must be fed through an ADC to be read by the microcontroller. The Arduino Uno's built-in ADC was used instead of the provided MLX90614 ADC chip, as they have comparable performance, which simplifies the circuit. Referring to the datasheet of the Arduino Uno, it was found that it offers a 10-bit resolution with a 5V range by default, giving a resolution of 4.88mV. However, the Arduino's

analogue reference was changed to 3.3V (instead of the default 5V), giving a better resolution of 3.22mV (therefore reducing the digitisation error). In future experiments, an even lower reference voltage value could be used to achieve even lower digitisation error, provided that it is not lower than the highest expected output voltage of the sensors (to avoid clipping).

3.2. Circuitry Overview

When constructing the circuits, application circuits in datasheets were closely followed as a reference. Note that the type of capacitors used for decoupling was the MLCC type, as their performance is highly independent of temperature. Also note that the electronics were built on a breadboard rather than on a PCB for easy modification under tight time deadlines. While PCBs offer better layout control (therefore, higher SNR can be achieved), their fixed connections make “on-the-go” modifications impractical.

Analogue Sensor: The sensor’s Vout, Vs, and GND pins were connected to the Arduino Uno’s A0, 5V, and GND pins, respectively. A 0.1 uF decoupling capacitor was placed across pins Vs and GND of the sensor to attenuate supply voltage spikes, which could have affected temperature readings.

Digital Sensor: The sensor was used in its external power supply mode. This was achieved by connecting the “VDD” and “GND” pins to the 5V and GND pins of the Arduino, respectively. The “DQ” pin of the sensor was then connected to a GPIO pin of the Arduino with a $4.7\text{k}\Omega$ pull-up resistor connecting this line to the Arduino’s 5V pin.

RTD Sensor: The resistances of the Wheatstone bridge were chosen to be 1 kOhm to ensure a fully balanced bridge. When the temperature changes, the voltage difference across the lefthand channel and right hand channel is in the mV range, therefore an MCP6002 amplifier was connected to the circuit so that the Arduino MCU can read this value. A "Virtual GND" has been added to the amplifier so that the output voltage is not limited to 0V at low temperatures and a voltage that the ADC can read is output.

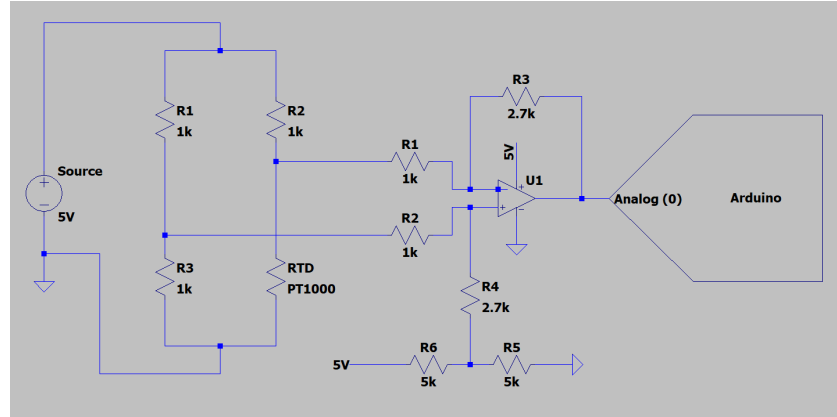


Figure 4. Readout circuit for RTD

IR Sensor: The ASSP (Signal Conditioning Application Process) digitises the IR thermopile output, using the 17-bit ADC of the IR. The sensor was interfaced directly to the microcontroller via the I²C bus, transmitting fully digitised temperature data. A decoupling capacitor is used to suppress high-frequency noise from the switching PSU and USB interface. Pull-up resistors are used on I²C buses because they utilise open-drain outputs, which only pull the lines low. Therefore, resistors are required to pull the lines high and to ensure proper logic transitions (Melexis 2013).

4. Software

The OneWire.h library was used for the digital sensor (*DS18B20*), for the IR sensor (*MLX90614*) it was Adafruit_*MLX90614.h*, and *TMP36.h* for the analogue sensor (*TMP36*). Adjustments were made to the example codes to specify the interval at which sensor readings were taken.

Note that the outputs were not filtered; therefore, small measurement errors were expected due to the finite SNR of the developed readout system. Analysis on the recorded measurements was conducted using Excel and MATLAB - see public GitHub repository.

5. Sensor Reading Analysis

5.1. Analogue Sensor

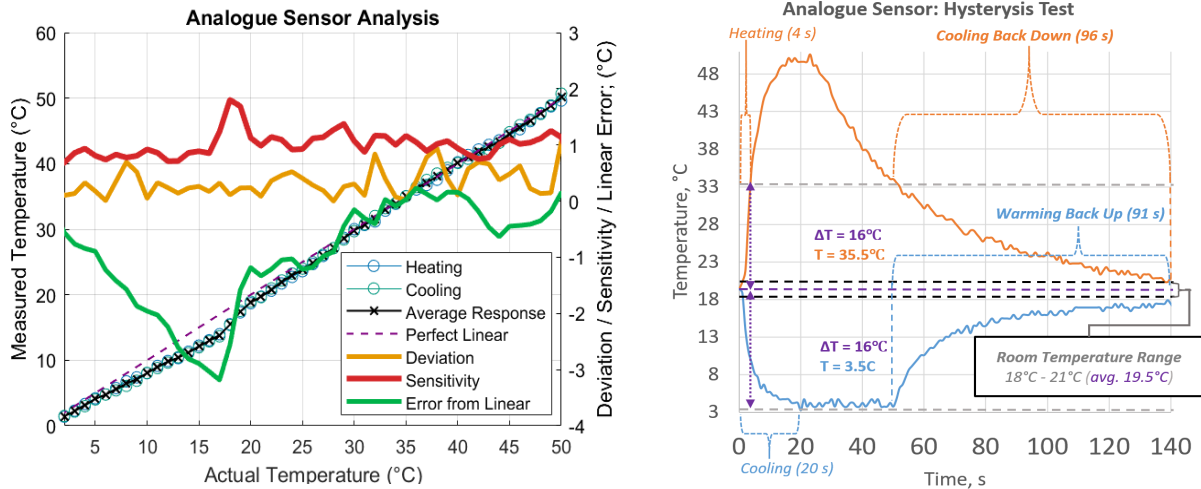


Figure 5. Analogue Sensor Readings (RHS: Hysteresis Test, LHS - all other data)

Accuracy (Fig. 5, LHS): the measured error (see “Error from Linear”) ranged from +0.23°C (@36°C), to -3.1°C (@17°C). In comparison, the accuracy listed in the datasheet is $\pm 2^\circ\text{C}$. (Analog Devices 2015). Interestingly, the measured error was negative throughout almost the entire temperature range. It is probable that additional errors were caused by test bench imperfections (e.g., poor insulation to the surrounding environment).

Sensitivity (Fig. 5, LHS): ideal sensitivity (gradient of “Average Response”) would be $1^\circ\text{C}_{\text{meas}}/\text{°C}$, though in practice, it ranged from $0.68^\circ\text{C}_{\text{meas}}/\text{°C}$ (@2°C) to $1.80^\circ\text{C}_{\text{meas}}/\text{°C}$ (@18°C). Sensitivity conversion to units of mV/°C can be performed using the sensor’s 10mV/°C scale factor (Analog Devices 2015). This gives a sensitivity range of 6.8mV/°C to 18mV/°C.

Linearity (Fig. 5, LHS): a perfectly linear sensor would have sensitivity of $1^\circ\text{C}_{\text{meas}}/\text{°C}$, though this was not the case in practice as described in the previous paragraph (and as seen in Fig. 4, LHS).

Response Time (Fig. 5, RHS): the following two arbitrary temperature steps were timed: a transition from room temperature (19.5°C) to $(19+16)^\circ\text{C}=35.5^\circ\text{C}$ took 4s, and a transition from room temperature (19.5°C) to $(19.5-16)^\circ\text{C}=3.5^\circ\text{C}$ took 20s. Though this difference is largely due to differences in heater & cooler powers, rather than sensor limitations.

Hysteresis (Fig. 5, RHS): it was found that it takes the sensor 91s to warm back up from 3.5°C to room temperature (16°C) in ambient air, while cooling back down from 35.5°C to room temperature in ambient air takes 96s. Though both values settle back to room temperature - meaning there is no hysteresis provided a long enough time period.

Precision (Fig. 6): for an accurate evaluation of the sensor’s precision, a high number of temperature sweeps should be recorded. Throughout this lab work, a total of three runs were carried out (more runs should have been conducted). These runs are plotted in Figure 5. The difference between the highest temperature reading of the sensor and the lowest temperature reading of the sensor at a specific “actual temperature” across these runs was computed - see “MaximumDeviation” plotline. The maximum deviation was found to be 1.7°C , closely corresponding to the 2°C accuracy given in the datasheet of the sensor (Analog Devices 2015).

Stability (Fig. 6): stability could be partly characterised via inspection of the “Maximum Deviation” plotline in Figure 5, as it shows *how different* the readings among unique runs were at a specific “actual” temperature. Though a stability evaluation method similar to one used for characterising the digital sensor should have been used for a more accurate characterisation.

Environmental Robustness: Throughout the experiment, the sensor did not seem to get damaged in any significant way due to excessive temperatures. It should be noted, however, that the sensor comes in a TO-92 package, the leads of which can be accidentally snapped off if proper caution is not taken. (Analog Devices 2015) This is exactly what happened when trying to connect up the sensor using

independent jumper wires - a replacement was then sourced. A JST connector with a pitch matching that of the sensor was found to be less prone to such damage, which is caused by mechanical force

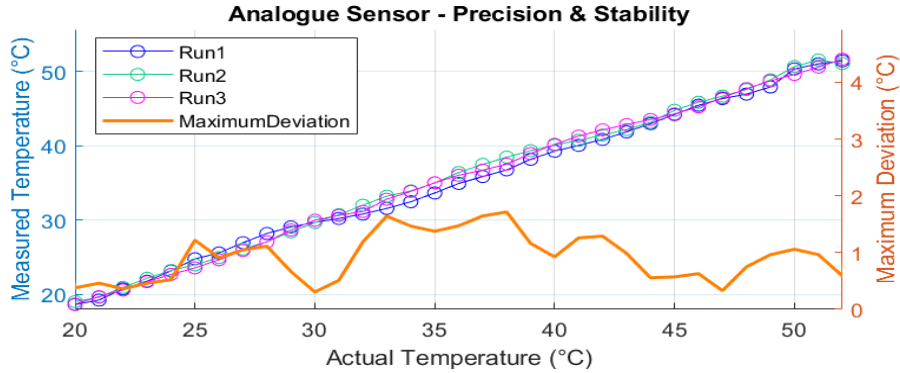


Figure 6. Analogue Sensor Readings and Analysis Regarding Precision and Stability).

5.2. Digital Sensor

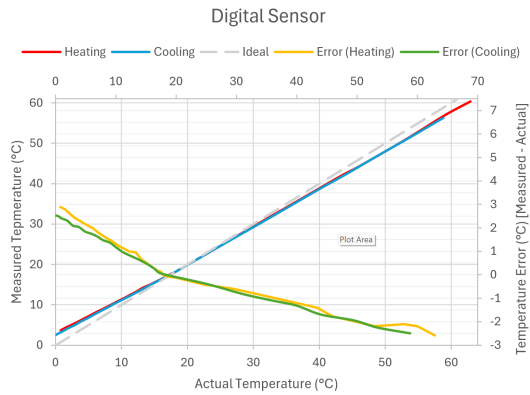


Figure 7. Digital Sensor Readings

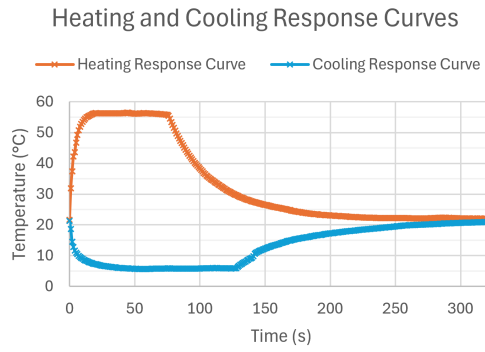


Figure 8. Heating and Cooling Response

Accuracy: As shown in Figure 7, when at room temperature (17.5°C), the error was 0°C , however, it increases linearly (by a different factor depending whether above or below room temperature) as the temperature is controlled away from room temperature. The error showed that the digital sensor read a temperature that was higher than reality when below room temperature, and lower than reality when above room temperature, implying the system is reluctant to deviate from room temperature. This is not a result of thermal lag, it was ensured that the temperature settled before taking readings. Additionally thermal lag would cause the error to be of opposing polarity between heating and cooling which is not the case. The maximum error was $\pm 3^{\circ}\text{C}$ (higher than the quoted “ $\pm 0.5^{\circ}\text{C}$ Accuracy” (Maxim Integrated 2019)). However, this error is proportional to the deviation from room temperature, meaning it is likely a systematic error from the test bench, likely a result of poor thermal insulation.

Sensitivity: The digital sensor outputs a value, $^{\circ}\text{C}_{\text{meas}}$, so the sensitivity is given as “ $^{\circ}\text{C}_{\text{meas}}/\text{°C}$ ”. Above room temperature the sensor had a sensitivity of $0.94^{\circ}\text{C}_{\text{meas}}/\text{°C}$, and $0.85^{\circ}\text{C}_{\text{meas}}/\text{°C}$ for below, this difference can be attributed to the change in test bench setup. Whilst these differ from the ideal $1^{\circ}\text{C}_{\text{meas}}/\text{°C}$, this error is most likely a result of the poor thermal insulation of the sensor from the surrounding environment as opposed to the sensor itself.

Linearity: Figure 7 shows that the digital sensor has a very strong linear relationship. Again, the slight change in gradient across room temperature due to the change in test bench setup (switching between the Peltier cooler and Heating Element) altering the dynamics of the surrounding environment.

Hysteresis: Our results show little-to-no effect from hysteresis. The slight discrepancy between the heating and cooling below room temperature testing, is more likely a result from a change in room temperature/surrounding environment rather than a property of the digital sensor.

Response Time: Figure 8 shows the response time curves for sudden changes in temperature of the digital sensor. Below shows how long the sensor took for (approximately) equal temperature changes.

Sensor on Test Bench:

- 21.31°C to 5.69°C (-Δ15.62°C) in 50s
- 42.19°C to 56.25°C (+Δ14.06°C) in 16s

Returning to Room Temperature:

- 5.88°C to 21°C (+Δ15.12°C) in 196s
- 37.38°C to 22°C (-Δ15.38°C) in 199s

The sensor returns to ambient in the same amount of time independent of being above or below ambient. However, the resistive heater was much faster heating up the sensor than the Peltier module was at cooling it down. This could have been due to the resistive heater operating at a higher power (5W) than the peltier cooler (0.75W) and so can deliver more power to cause a change in temperature.

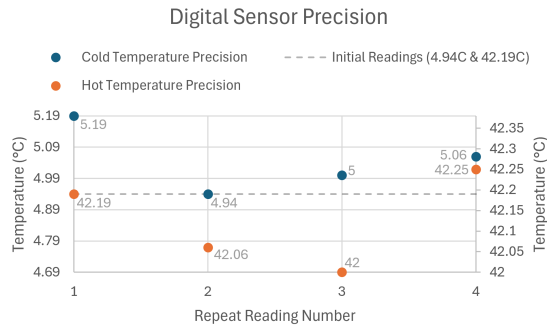


Figure 9. Digital Sensor Results from Precision Testing

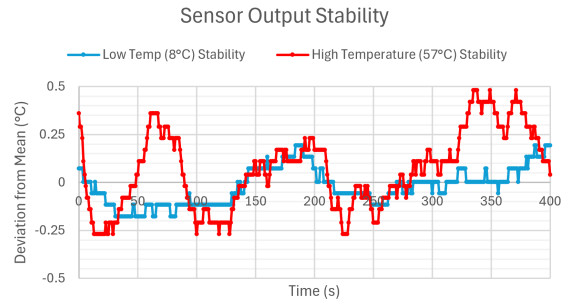


Figure 10. Digital Sensor Results from Stability Testing

Precision: The test bench was maintained at a set temperature by referencing the “Golden Standard” probe. Initial readings with the digital sensor were taken (grey dashed line), and then four subsequent readings were taken (digital sensor was removed in between measurements and allowed to return to room temperature) and compared to the initial reading in Figure 9. The sensor demonstrates a very high precision as the maximum deviation between the tests was ±0.25°C. A higher resolution “Golden Standard” probe could have led to better results as it only displays 1.d.p., meaning that there is potential for error in the maintained temperature.

Stability: The test bench was maintained at a set temperature using the “Golden Standard” probe and readings from the digital sensor were taken every second. Figure 10 shows that over the course of 400 seconds the readings oscillated within ±0.5°C of the means, and there was no drift in the sensor.

Environmental Robustness: The digital sensor demonstrated poor environmental robustness due to deviations in the ambient temperature or airflow causing its readings to change. This could be resolved by calibrating the sensor for the specific ambient temperature, or if this is not feasible, improving the test bench to further isolate it from the surrounding environment. Additionally insufficient mounting pressure reduced the accuracy of readings.

Resolution: In our testing the resolution was found to be 0.06°C, however, it was later found out that the Arduino outputs just 2 decimal places by default which explains the difference between our value and its datasheet value of 0.0625°C (Maxim Integrated 2019).

5.3. RTD Sensor

Accuracy: As can be seen from the yellow line, it shows an error of approximately -3.8°C around 0°C. Between 40°C and 70°C degrees, the error is positive. However, after 70°C, it seems that the error tends to go negative. During cooling, it was positive.

Precision: Before measuring the temperature with the sensor for the final graphs, measurements were taken repeatedly between 0-100°C. Since this sensor belongs to class A, its precision is at a high level. Because platinum is a non-reactive material. The precision obtained from the measurements is 0.2°C. This value may vary depending on the measurement scheme and parameters such as cable resistance.

Sensitivity: The nominal sensitivity of the PT1000 is $3.85\Omega/\text{°C}$ (Adafruit, n.d.). However, as can be seen in the graph, there are sometimes deviations (max ±4°C) and these completely stem from the circuit.

Linearity: Figure 11 shows that the red line in the heating and the blue line in the cooling measurements is very close to the ideal straight line and the sensor has high linearity.

Hysteresis: When the temperature changes, the glass and metal housing parts surrounding the platinum element expand and contract at different rates due to different thermal expansion coefficients. As illustrated in Figure 11 RH, the largest hysteresis difference is between 30-50°C.

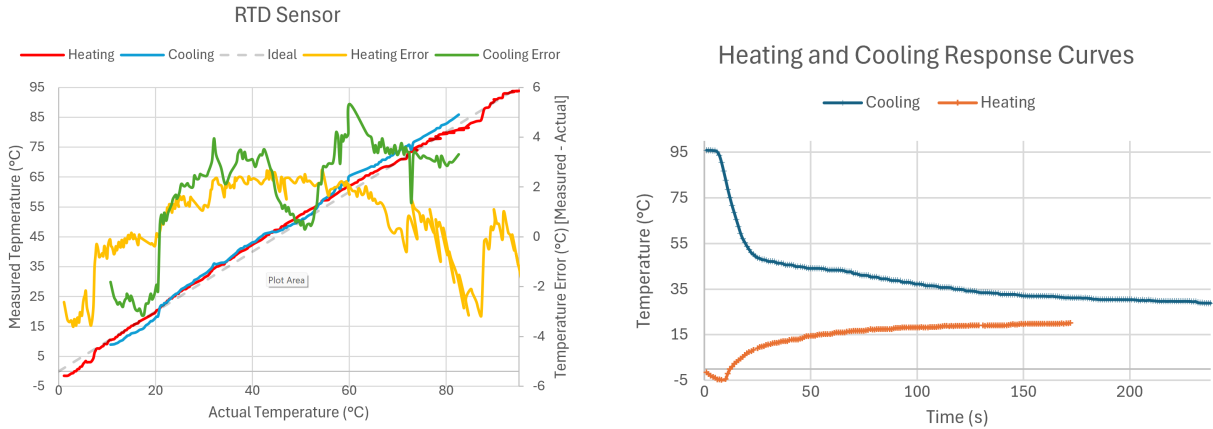


Figure 11. RTD Sensor Readings (RHS: Heating/Cooling Response Curves, LHS - all other data)

Stability: The PT series are known for their high stability. Loss of stability is caused by factors such as mechanical damage and thermal shock. If the sensor is frequently subjected to wide heating and cooling cycles, the internal voltage will change over time.

Environmental Robustness: If the RTD sensor circuit has a good hermetic protection, it is quite resistant to environmental factors such as temperature, humidity, electromagnetic fields, vibration. The sensor maintains its performance even in water and is able to work at higher temperatures (up to 400-850°C). The points to pay attention to are the selection of quality wires, resistors and a suitable amplifier model for the circuit. With precise adjustments, it is possible to maximize sensitivity.

5.4. IR Sensor

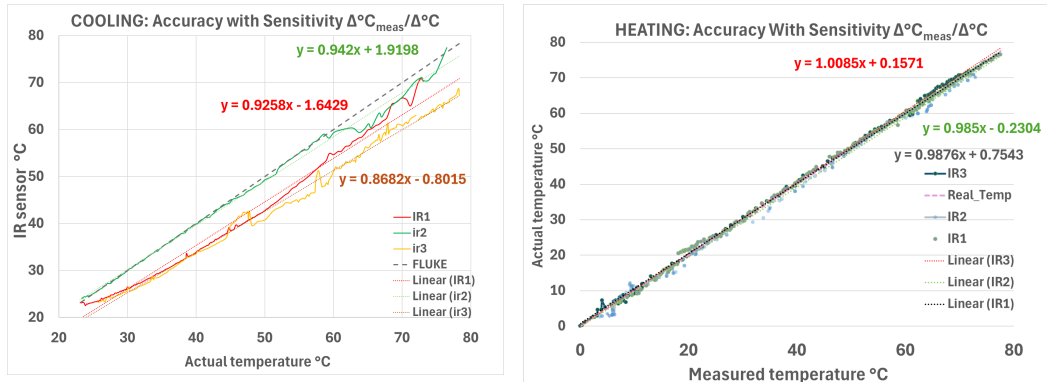


Figure 12: IR sensor readings testing precision and Hysteresis curve

Accuracy & Sensitivity: Across the three heating runs from 0°C to 80°C, the accuracy curves are highly consistent, with noticeable differences only at the temperature extremes [Figure 14]. For the sensor to be considered functioning, each run must remain within the acceptable ± 3 °C range specified in the datasheet and exhibit similar sensitivity behaviour. Between approximately 17°C and 30°C, the error for both heating and cooling approaches zero, aligning with the MLX90614's stated ± 0.5 °C accuracy in this region. The deviation of the cooling test bench is greater than that of the heating test bench. This could be because the sensor window was unshielded during the cooling experiment, whereas it was encased in a plastic sheath during the heating experiment. Moisture on the sensor window can reduce IR transmission and increase negative error. Regarding the sensitivity derivations, it can be seen that the sensor is highly sensitive to absolute temperature, with a sensitivity range of $0.89 \text{ }^{\circ}\text{C}_{\text{meas}}/\text{ }^{\circ}\text{C}$ to $1.0085 \text{ }^{\circ}\text{C}_{\text{meas}}/\text{ }^{\circ}\text{C}$, indicating a near-unity response. This indicates that the MLX90614 responds nearly linearly to changes in temperature across the tested range.

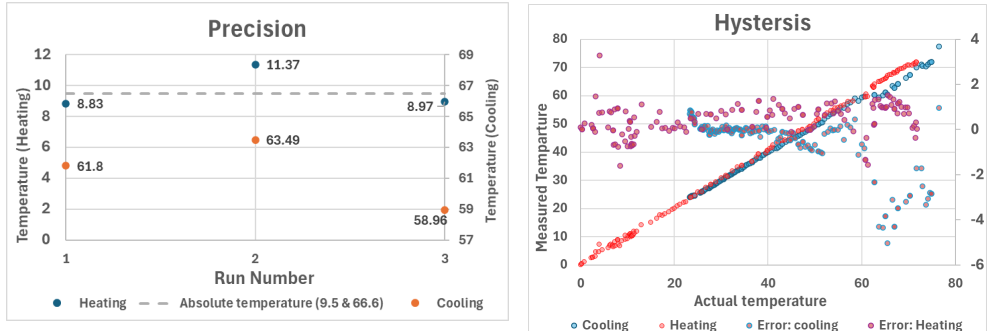


Figure 13: IR sensor readings testing precision and Hysteresis curve

Precision & Environmental Robustness: Across three runs, two temperature points were recorded, which were repeated in each run. For the heating test bench, the absolute temperature was 9.5°C, with an error range of -0.67°C to 1.87°C. For the cooling test bench, the datapoint was 66.6°C, with a measured error of -3.11°C to -7.64°C. According to the datasheet, temperature outputs are provided with a digital resolution of 0.02°C via the SMBus and is calibrated over a wide operating range (ambient -40°C to +125°C; object -79°C to +380°C), with a stated accuracy of $\pm 0.5^\circ\text{C}$ around room temperature. The errors for both test benches lie outside the nominal accuracy range, indicating potential issues with the test bench design rather than the sensor. Because the MLX90614 relies on radiative heat flux, its performance is significantly influenced by environmental stability and the design of the test bench. Although the sensor includes an optical filter and the beaker was wrapped in black material to reduce stray radiation from the environment, remaining measurement errors can be attributed to condensation on the lens, thermal gradients across the medium (stirring was infrequent), or angular misalignment of the sensor's field of view caused by minor movement during stirring. These factors collectively explain the observed deviations and highlight the importance of a controlled and stable experimental setup for accurate MLX90614 measurements.

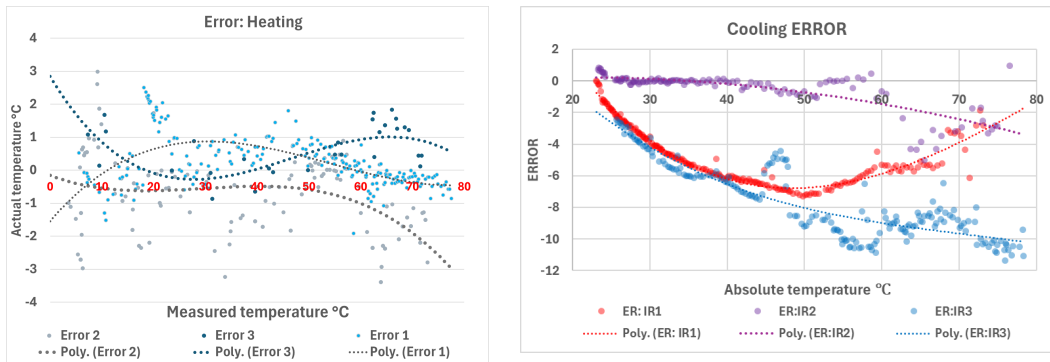


Figure 14: IR sensor errors (most deviation at temperature extremes)

Hysteresis: The plot above compares two of the best runs in terms of sensitivity, overlaying the heating and cooling curves. Consistent with the observations in the Accuracy and Sensitivity section, most of the error is concentrated at the temperature extremes. The cooling test bench did not go below 20°C, which accounts for the missing data points; however, between 20°C and 60°C, the sensor exhibits ideal behaviour, with minimal differences between the heating and cooling curves. At higher temperatures, the agreement deteriorates, indicating the onset of hysteresis effects, likely due to thermal gradients, as well as environmental factors and poor design of the test bench.

Stability: The sensor was aimed at room-temperature water to measure if the output drifted over time. The readings remained fairly consistent, with a maximum deviation of $\pm 0.5^\circ\text{C}$ from the "Gold Standard" probe. This oscillation can be attributed to background noise and falls within the datasheet ratings, indicating that the sensor meets the specified performance. Error curves against absolute temperature were also examined to see any systematic bias/offset from the test bench or measurement environment. These curves indicate that inaccuracies primarily occur at temperature extremes rather

than through temporal drift, supporting the conclusion that the sensor is stable and reliable within the tested range.

6. Comparison Table of Measured Sensor Specifications

	Analogue	Digital	RTD	IR
Accuracy	$\pm 3^\circ\text{C}$	$\pm 3^\circ\text{C}$	$\pm 4^\circ\text{C}$	$\pm 6^\circ\text{C}$
Sensitivity	6.8-18mV/ $^\circ\text{C}$	$0.85\text{-}0.94^\circ\text{C}_{\text{meas}}/\text{mV}$	$3.85\Omega/\text{mV}$	High
Linearity	High	V. High	V. High	V. High
Hysteresis	None	None	None	None
Response Time	91s: $36^\circ\text{C} \rightarrow 20^\circ\text{C}$ 95s: $4^\circ\text{C} \rightarrow 20^\circ\text{C}$	196s: $5.88 \rightarrow 21^\circ\text{C}$ 199s: $37.38 \rightarrow 22^\circ\text{C}$	160s: $-5 \rightarrow 20^\circ\text{C}$ 125s: $36 \rightarrow 21^\circ\text{C}$	Instant
Precision	$\pm 1.7^\circ\text{C}$	$\pm 0.25^\circ\text{C}$	$\pm 0.2^\circ\text{C}$	High
Resolution	<i>ADC dependant</i>	0.06 $^\circ\text{C}$	<i>ADC dependant</i>	0.02 $^\circ\text{C}$
Stability	$\pm 1.7^\circ\text{C}$	High ($\pm 0.5^\circ\text{C}$)	High	High
Environmental Robustness	Medium	Low	High	Low

7. Work Allocation

	H. M.	T. R.	U. B.	M. B.
Digital Sensor	✓			
Analogue Sensor		✓		
RTD Sensor			✓	
IR Sensor				✓
Contact Test Bench	✓	✓	✓	
Non-contact Test Bench				✓

8. References

- Adafruit. n.d. "Platinum RTD Sensor - PT1000 - 3 Wire 1 meter long : ID 3984." Adafruit. Accessed December 12, 2025. <https://www.adafruit.com/product/3984#technical-details>.
- Analog Devices. 2015. "Data Sheet (TMP35/TMP36/TMP37)." https://www.analog.com/media/en/technical-documentation/data-sheets/tmp35_36_37.pdf.
- Heraeus Sensor Technology. n.d. "Platinum Resistance Temperature Detector." [3290+-+datasheet.pdf](https://cdn-shop.adafruit.com/product-files/3290/3290+-+datasheet.pdf). <https://cdn-shop.adafruit.com/product-files/3290/3290+-+datasheet.pdf>.
- Maxim Integrated. 2019. "DS18B20 Datasheet." DS18B20 Datasheet. <https://www.analog.com/media/en/technical-documentation/data-sheets/ds18b20.pdf>.
- Melexis. 2013. "MLX90614 family." Course Websites. <https://cdn-shop.adafruit.com/datasheets/MLX90614.pdf>.
- RS PRO. 2024. "Datasheet RS PRO Thermal grease, 1.8W/m K." <https://uk.rs-online.com/web/p/thermal-grease/2065707>.